

## Supporting information

### **Multipoint interactions enhanced H<sub>2</sub> storage and organosulfur removal in a microporous metal–organic framework**

**Wen-Wen He,<sup>a</sup> Shun-Li Li,<sup>b</sup> Wen-Liang Li,<sup>a</sup> Ji-Sen Li,<sup>b</sup> Guang-Sheng Yang,<sup>a</sup>  
Shu-Ran Zhang,<sup>a</sup> Ya-Qian Lan\*,<sup>b</sup> Ping Shen<sup>a</sup> and Zhong-Min Su\*<sup>a</sup>**

<sup>a</sup> Institute of Functional Material Chemistry, Faculty of Chemistry, Northeast Normal University, Changchun, 130024 Jilin, P. R. China. E-mail: zmsu@nenu.edu.cn.

<sup>b</sup> Jiangsu Key Laboratory of Biofunctional Materials, School of Chemistry and Materials Science, Nanjing Normal University, Nanjing, 210023, Jiangsu, P. R. China. E-mail: yqlan@njnu.edu.cn

## 1. Experimental Section

### S1. Materials and measurements

### S2. Synthesis of IFMC-16

### S3. X-ray crystallography

## 2. Figures

**Fig. S1** Illustration of the three-connected H<sub>3</sub>BPTC ligand and the two-connected H<sub>2</sub>BDC ligand, they have a nearly equal coordination length.

**Fig. S2** Space-filling representation of **IFMC-16** viewed from the [0 0 1] direction.

**Fig. S3** Ball-and-stick representations of the two right handed single helices in the channel of A.

**Fig. S4** (a) The N<sub>2</sub> gas-sorption isotherms for **IFMC-16**. The filled and open squares represent adsorption and desorption branches, respectively. (b) The pore size distribution of **IFMC-16**.

**Fig. S5** Isothermic heat of adsorption for hydrogen on **IFMC-16**.

**Fig. S6** (a) The H<sub>2</sub> gas-sorption isotherms for **IFMC-16** (77 K). (b) Comparison of H<sub>2</sub> isotherms at ambient pressure (77K) in **IFMC-16**: experimental data and simulated isotherm. (c) Comparison of H<sub>2</sub> isotherms at high pressure (77K) in **IFMC-16**: experimental data and simulated isotherm.

**Fig. S7** CO<sub>2</sub> sorption isotherms of **IFMC-16** at 273K and 298K.

**Fig. S8** Isothermic heat of adsorption for CO<sub>2</sub> on **IFMC-16**.

**Fig. S9** X-Ray powder diffraction patterns of activated **IFMC-16**, as-synthesized **IFMC-16** and simulated **IFMC-16**.

**Fig. S10** X-Ray powder diffraction patterns of regeneration **IFMC-16** (run 2), regeneration **IFMC-16** (run 1), **DBT@IFMC-16**, **BT@IFMC-16**, as-synthesized **IFMC-16** and simulated **IFMC-16**.

**Fig. S11** FT-IR spectra of fresh **IFMC-16**, activated **IFMC-16**, **BT@IFMC-16** and **DBT@IFMC-16** at room temperature.

**Fig. S12** TGA curves of **IFMC-16**.

**Fig. S13** TGA curves of **BT@IFMC-16** and **DBT@IFMC-16**.

**Fig. S14** UV-Vis spectra for (a) **BT@IFMC-16** and (b) **DBT@IFMC-16** during the regeneration experiments.

## 3. Tables

**Table S1** Crystal data and structure refinements for compound **IFMC-16**.

**Table S2** The adsorption amount of **IFMC-16** for BT and DBT in different concentration.

**Table S3** Surface area, pore volume and N<sub>2</sub> uptake for **IFMC-16**, regenerated **IFMC-16**, **BT@IFMC-16** and **DBT@IFMC-16**.

## 4. Scheme

**Scheme S1** Multipoint interaction sites in the framework of **IFMC-16**.

## Experimental Section

### S1. Materials and measurements

All chemical materials were purchased from commercial sources and used without further purification. The FT-IR spectra were recorded from KBr pellets in the range 4000–400  $\text{cm}^{-1}$  on a Mattson Alpha-Centauri spectrometer. The phase purities of the bulk samples were identified by X-ray powder diffraction on a Rigaku, Rint 2000 diffractometer. The UV-Vis absorption spectra were examined on a Shimadzu UV-2550 spectrophotometer in the wavelength range of 200–800 nm. The C, H, and N elemental analyses were conducted on a Perkin-Elmer 240C elemental analyzer. TGA was performed on a Perkin-Elmer TG-7 analyzer heated from room temperature to 1000 °C at a ramp rate of 5 °C/min under nitrogen. The  $\text{N}_2$ ,  $\text{H}_2$  and  $\text{CO}_2$  sorption measurements were performed on automatic volumetric adsorption equipment (Micromeritics ASAP2050). Before gas adsorption measurements, the sample was immersed in methanol for 72 h, and the extract was decanted. Fresh methanol was subsequently added, and the crystals were allowed to stay for an additional 24 h to remove the nonvolatile solvates. The sample was collected by decanting and treated with dichloromethane similarly to remove methanol solvates. After the removal of dichloromethane by decanting, the sample was activated by drying under a dynamic vacuum at room temperature overnight. Before the measurement, the sample was dried again by using the ‘outgas’ function of the surface area analyzer for 12 h at 90 °C. The samples including organosulfur compounds were analyzed by gas chromatography (Shimadzu GC-2014 system by using a G-100 column (40 m methyl silicone with an ID of 1.2 mm and 1.0  $\mu\text{m}$  film thickness: Chemicals Evaluation and Research Institute, Japan) coupled with a flame ionization detector (GC-FID). The conditions were as follows: injection temperature 553 K, detector temperature 553 K, oven temperature 453 K, carrier gas : He (20  $\text{mL}\cdot\text{min}^{-1}$ ), sample injection volume 1  $\mu\text{L}$ .

### **Organosulfur adsorption experiment**

A liquid-phase adsorption experiment was carried out at 298 K in 2 mL glass vials filled with adsorbent (0.020 g) and a solution of isooctane (1 mL) including benzothiophene or dibenzothiophene with different concentrations. Then, the vials were agitated on a shaker at 150 rev min<sup>-1</sup> for 12 h. The adsorptive procedure was monitored by UV/Vis spectroscopy. The final isooctane solution, after removing the solid adsorbents, was analyzed by GC-FID. The solid **BT@IFMC-16** and **DBT@IFMC-16** (IFMC-16 with adsorbed BT or DBT molecules) was removed from the solution by filtration, the solvent of which was removed by keeping under vacuum at 393 K overnight, and dried in a desiccator.

### **Regeneration experiment**

The sample of **BT@IFMC-16** or **DBT@IFMC-16** was soaked in isooctane (5 mL), and replaced with fresh isooctane (5 mL) six times in 10 h. The regeneration procedure was monitored by UV/Vis for each washed isooctane and GC-FID measurements performed for the isooctane with BT or DBT.

## S2. Synthesis of IFMC-16

Cu(NO<sub>3</sub>)<sub>2</sub>·3H<sub>2</sub>O (0.109 g, 0.45 mmol), H<sub>3</sub>BPTC (0.028 g, 0.1 mmol), HPBA (0.060 g, 0.3 mmol) were dissolved in a mixture of DMF, CH<sub>3</sub>OH and H<sub>2</sub>O (5:1:1) and then 2 drops of HF were added. The mixture was placed in a Teflon reactor and heated at 85 °C for 3 days, and then it was gradually cooled to room temperature. The crystals were obtained in a 52% yield. Elemental microanalysis for [Cu<sub>4</sub>(BPTC)<sub>2</sub>(PBA)<sub>2</sub>(H<sub>2</sub>O)<sub>2</sub>]·12DMA·8CH<sub>3</sub>OH·6H<sub>2</sub>O, calculated (%): C, 49.63; H, 6.92; N, 7.37. Found (%): C, 48.78; H, 6.65; N, 7.02. IR (cm<sup>-1</sup>): 3429.87 (m), 2934.14 (w), 1634.93 (s), 1406.69 (s), 1400.42 (s), 1262.00 (m), 1185.66 (m), 1106.59 (w), 1066.58 (w), 1013.67 (s), 839.38 (w), 769.67 (s), 729.25 (w), 593.77 (m), 514.31 (m), 474.45 (s).

### S3. X-ray crystallography

Single-crystal X-ray diffraction data for **IFMC-16** was recorded by using a Bruker Apex CCD diffractometer with graphite-monochromated Mo-K $\alpha$  radiation ( $\lambda = 0.71069 \text{ \AA}$ ) at 293 K. Absorption corrections were applied by using a multi-scan technique. All the structures were solved by Direct Method of SHELXS-97 and refined by full-matrix least-squares techniques using the SHELXL-97 program within WINGX. Non-hydrogen atoms were refined with anisotropic temperature parameters. The SQUEEZE program implemented in PLATON was used to remove these electron densities for **IFMC-16**. Thus, all of electron densities from free solvent molecules have been “squeezed” out.

The detailed crystallographic data and structure refinement parameters for **IFMC-16** are summarized in Table S1.

**Table S1** Crystal data and structure refinements for compound **IFMC-16**.

Identification code	<b>IFMC-16</b>
formula	C <sub>110</sub> H <sub>184</sub> N <sub>14</sub> O <sub>44</sub> Cu <sub>4</sub>
Formula weight	2659.76
Crystal system	Tetragonal
Space group	<i>P</i> 4 <sub>1</sub>
<i>a</i> (Å)	26.070(5)
<i>b</i> (Å)	26.070(5)
<i>c</i> (Å)	18.601(5)
$\alpha$ (°)	90.00
$\beta$ (°)	90.00
$\gamma$ (°)	90.00
<i>V</i> (Å <sup>3</sup> )	12642(5)
<i>Z</i>	4
<i>D</i> <sub>calcd.</sub> [g cm <sup>-3</sup> ]	2.049
<i>F</i> (000)	7584
Reflections collected	64201 / 21703
<i>R</i> (int)	0.0596
Goodness-of-fit on <i>F</i> <sup>2</sup>	1.127
<i>R</i> <sub>1</sub> <sup>a</sup> [ <i>I</i> > 2 $\sigma$ ( <i>I</i> )]	0.0795
<i>wR</i> <sub>2</sub> <sup>b</sup>	0.2109

$$^a R_1 = \sum ||F_o| - |F_c|| / \sum |F_o|. \quad ^b wR_2 = \sqrt{\sum w(|F_o|^2 - |F_c|^2) / \sum w(F_o^2)^2}^{1/2}.$$

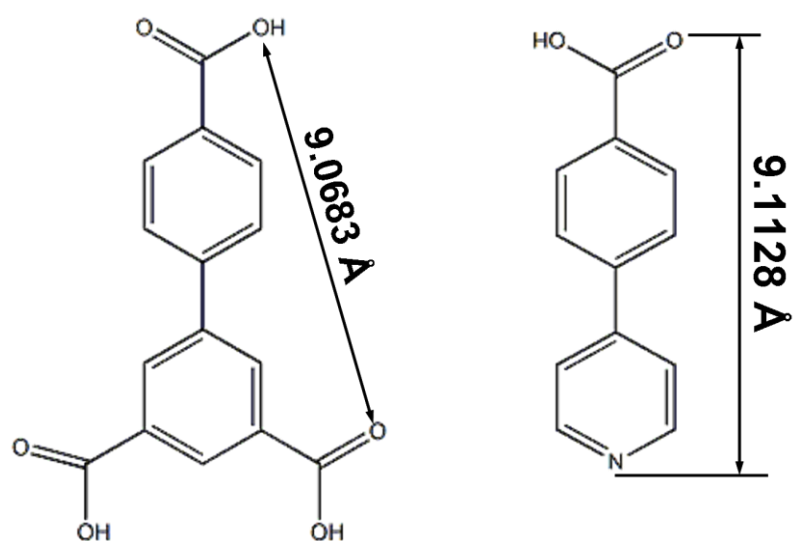


**Fig. S1** Illustration of the three-connected H<sub>3</sub>BPTC ligand and the two-connected H<sub>2</sub>BDC ligand, they have a nearly equal coordination length.

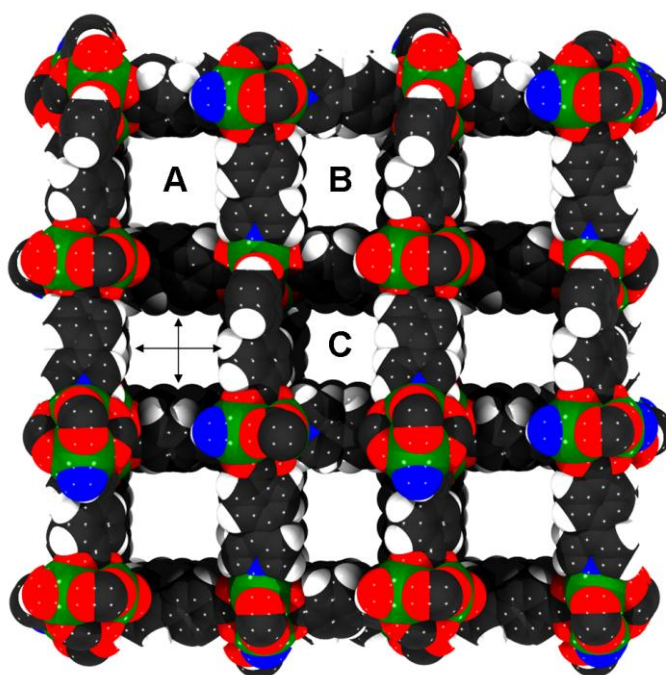


**Fig. S2** Space-filling representation of IFMC-16 viewed from the [0 0 1] direction. The corresponding sizes of channels A, B and C are  $13.1 \times 13.1 \text{ \AA}$ ,  $13.6 \times 12.7 \text{ \AA}$  and  $12.5 \times 12.5 \text{ \AA}$ , respectively.

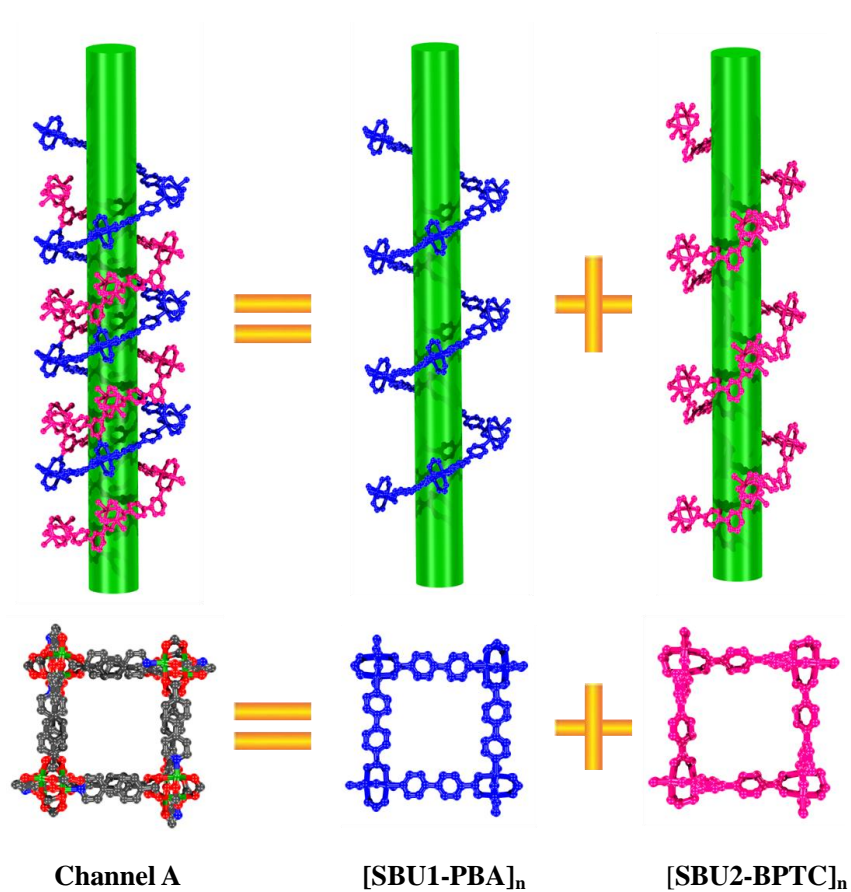
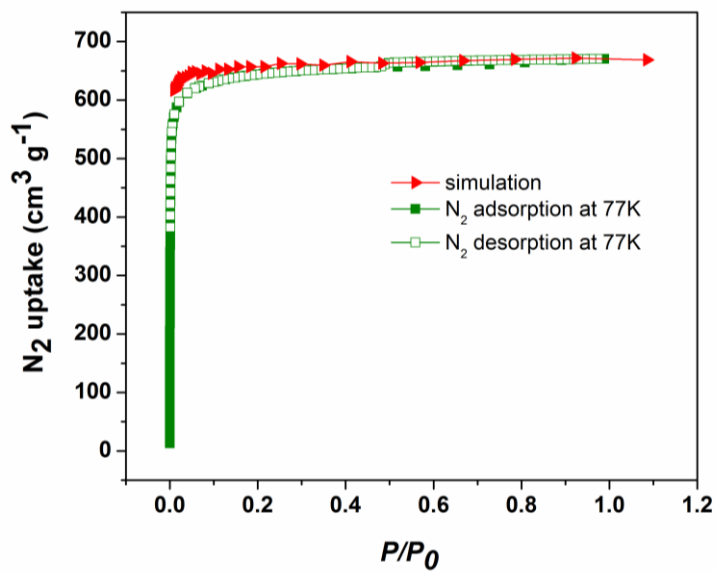
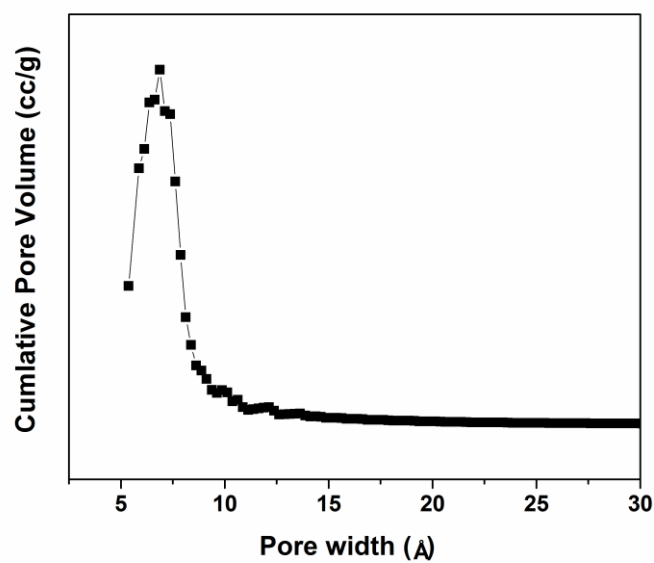


**Fig. S3** Ball-and-stick representations of the two right handed single helices in the channel of A.



(a)



(b)

**Fig. S4** (a) The N<sub>2</sub> gas-sorption isotherms for **IFMC-16** (77 K): experimental data (green) and simulated isotherm (red). (b) The pore size distribution of **IFMC-16** (analysis by HK method).

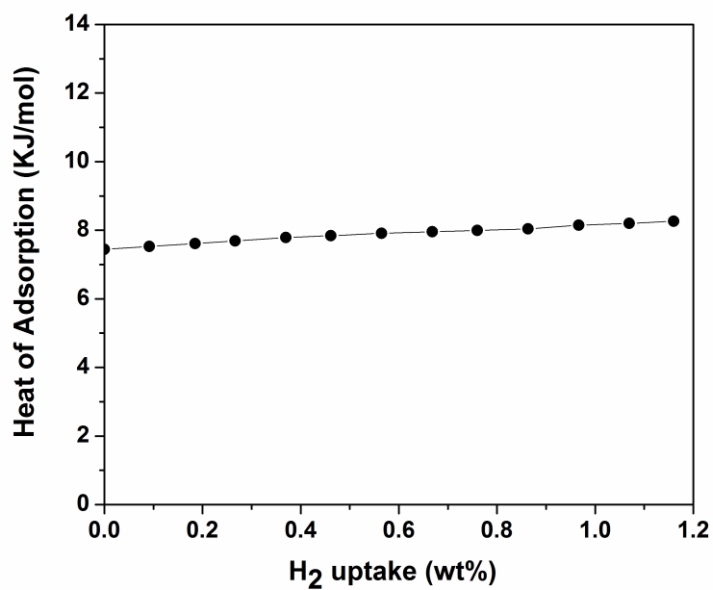
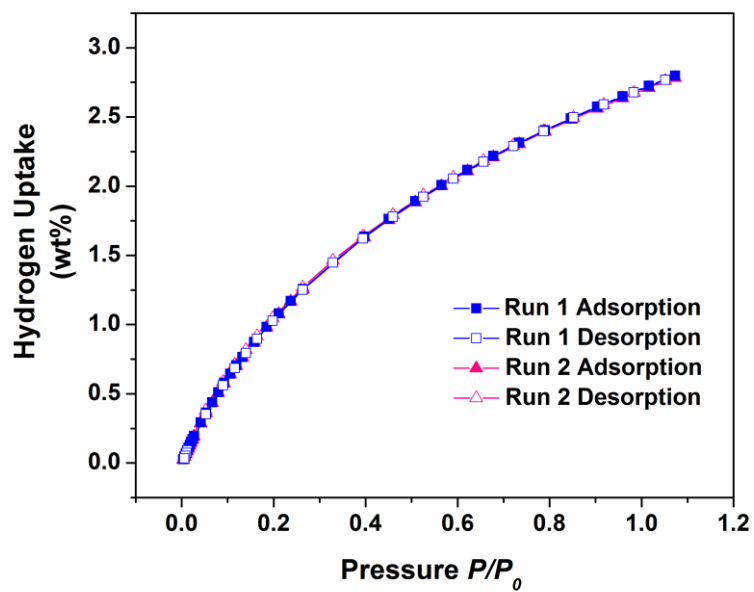
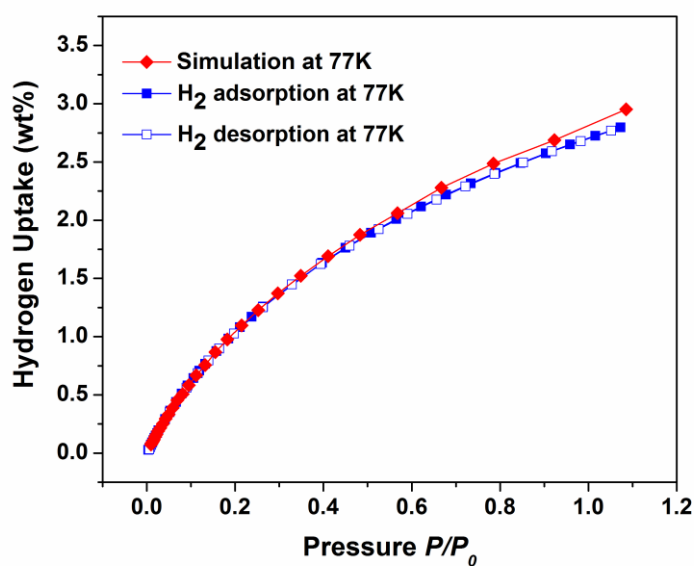


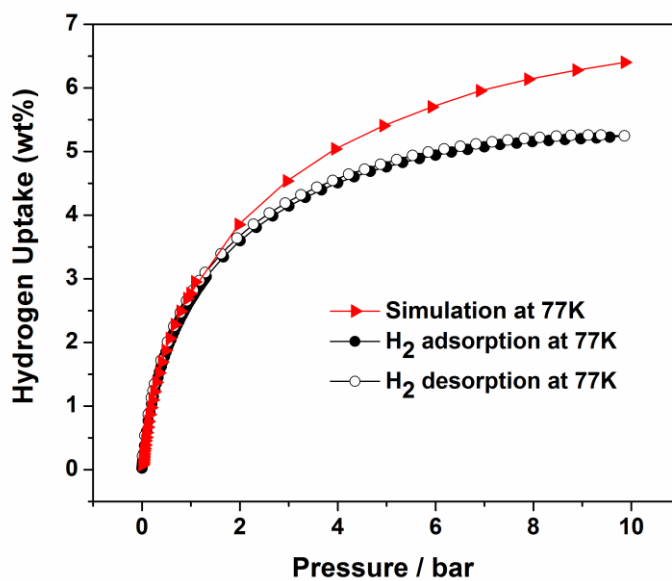
**Fig. S5** Isosteric heat of adsorption for hydrogen on **IFMC-16** (using the isotherms at 77 K and 87 K).



(a)



(b)



(c)

**Fig. S6** (a) The H<sub>2</sub> gas-sorption isotherms for **IFMC-16** (77 K). (b) Comparison of H<sub>2</sub> isotherms at ambient pressure (77K) in **IFMC-16**: experimental data (blue) and simulated isotherm (red). (c) Comparison of H<sub>2</sub> isotherms at high pressure (77K) in **IFMC-16**: experimental data (black) and simulated isotherm (red).

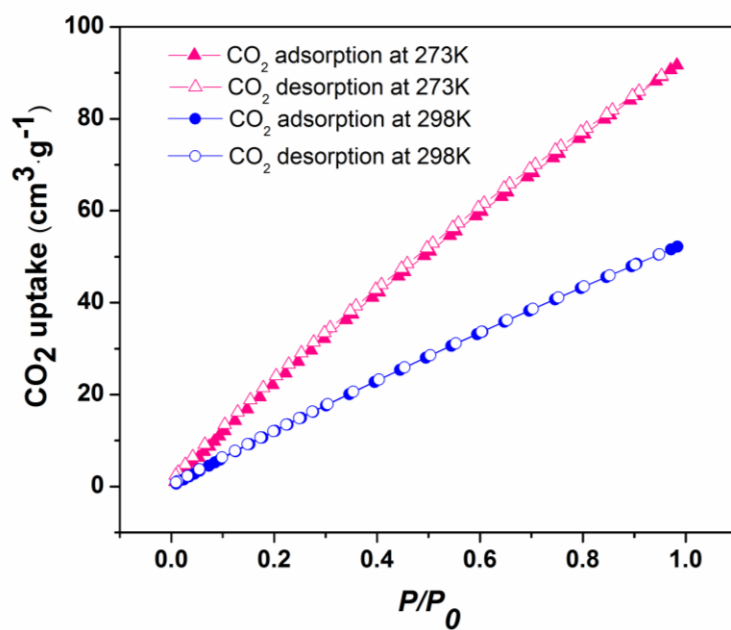


**Fig. S7** CO<sub>2</sub> sorption isotherms of **IFMC-16** at 273K (pink) and 298K (blue).

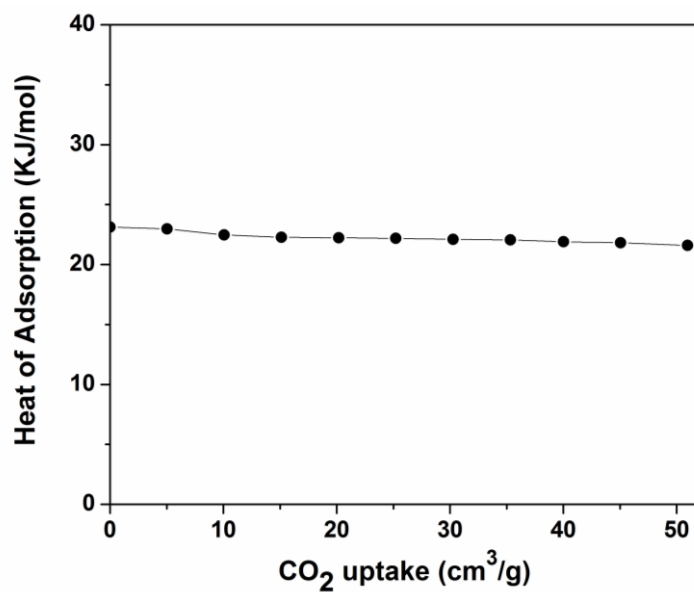
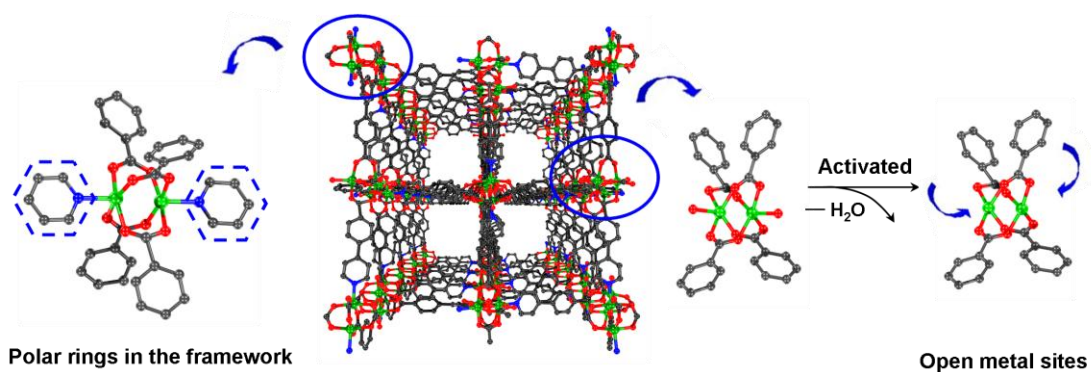


**Fig. S8** Isothermic heat of adsorption for CO<sub>2</sub> on **IFMC-16** (using the isotherms at 273 K and 298 K).



**Scheme S1** Multipoint interaction sites in the framework of **IFMC-16**.

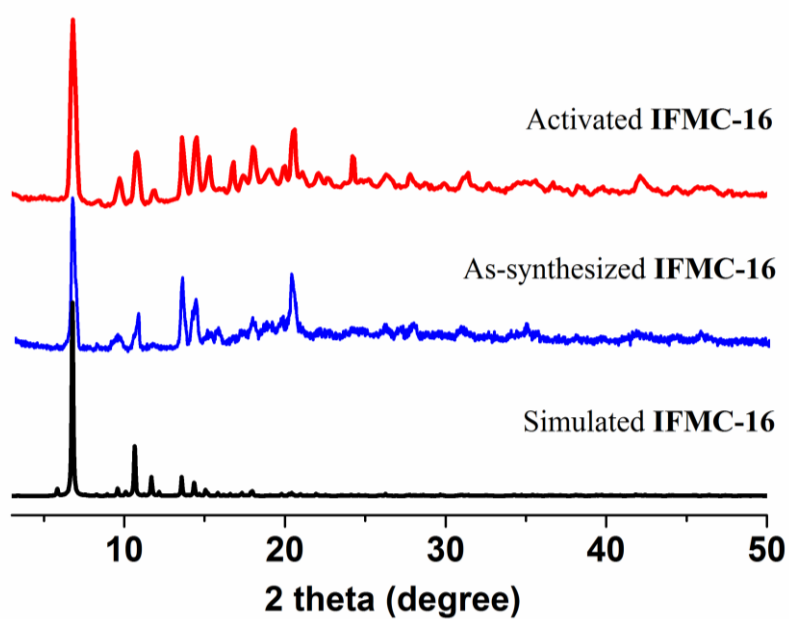


**Fig. S9** X-Ray powder diffraction patterns of activated **IFMC-16** (red), as-synthesized **IFMC-16** (blue) and simulated **IFMC-16** (black).

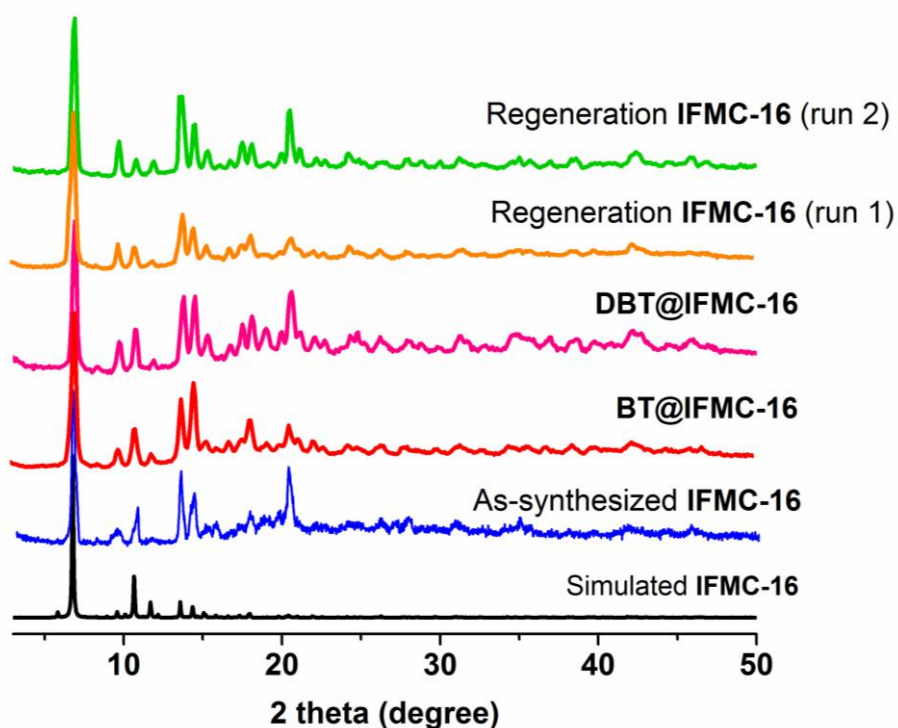


**Fig. S10** X-Ray powder diffraction patterns of regeneration **IFMC-16** (run 2) (green), regeneration **IFMC-16** (run 1) (orange), **DBT@IFMC-16** (pink), **BT@IFMC-16** (red), as-synthesized **IFMC-16** (blue) and simulated **IFMC-16** (black).

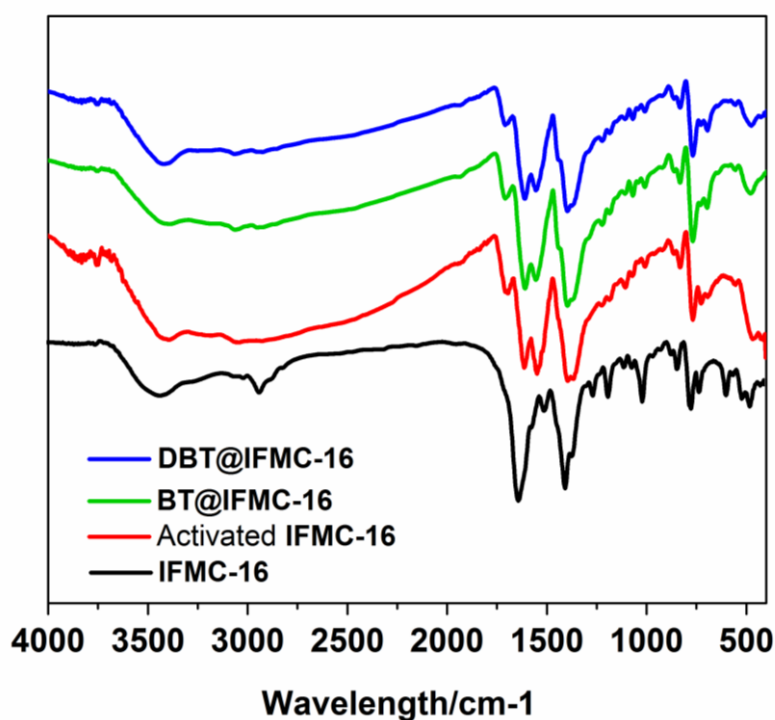


**Fig. S11** FT-IR spectra of fresh **IFMC-16**, activated **IFMC-16**, **BT@IFMC-16** and **DBT@IFMC-16** at room temperature.

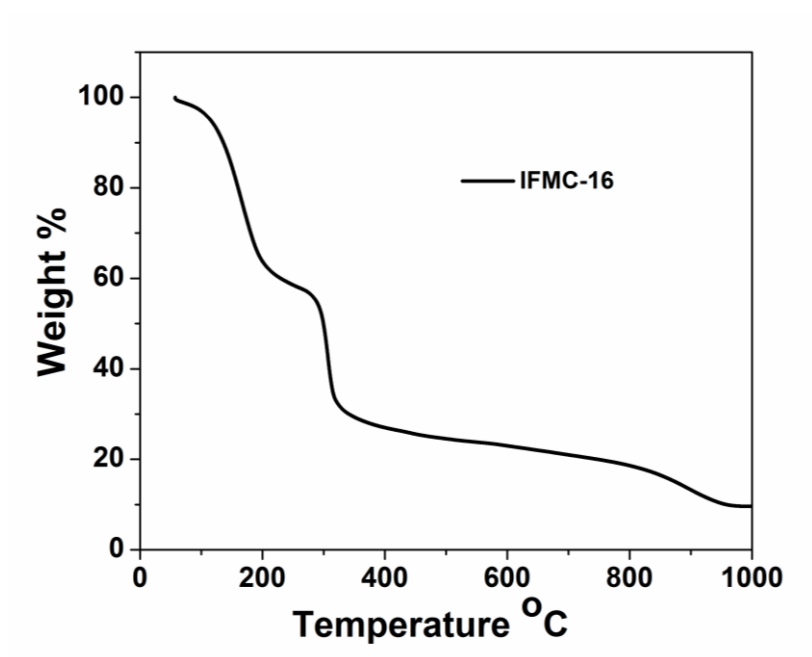


Fig. S12 TGA curves of IFMC-16.

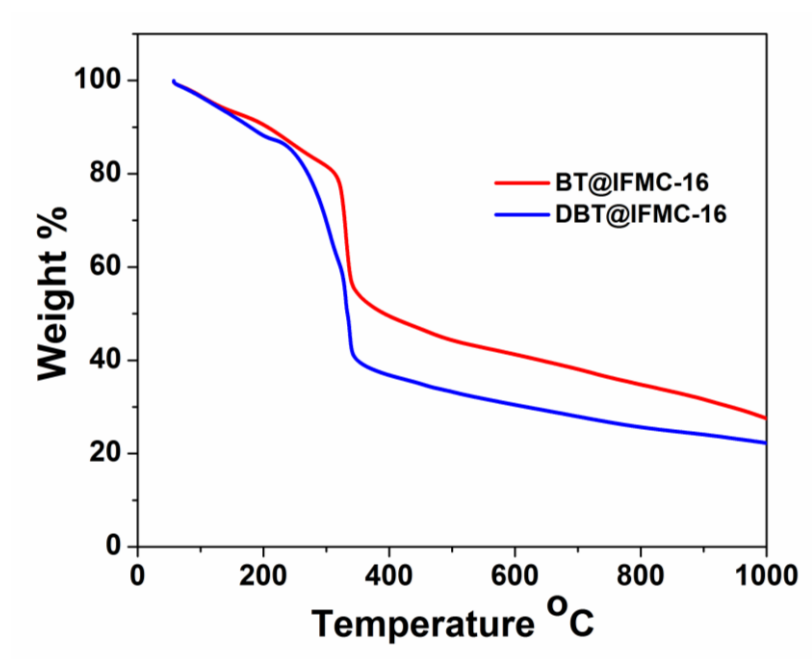
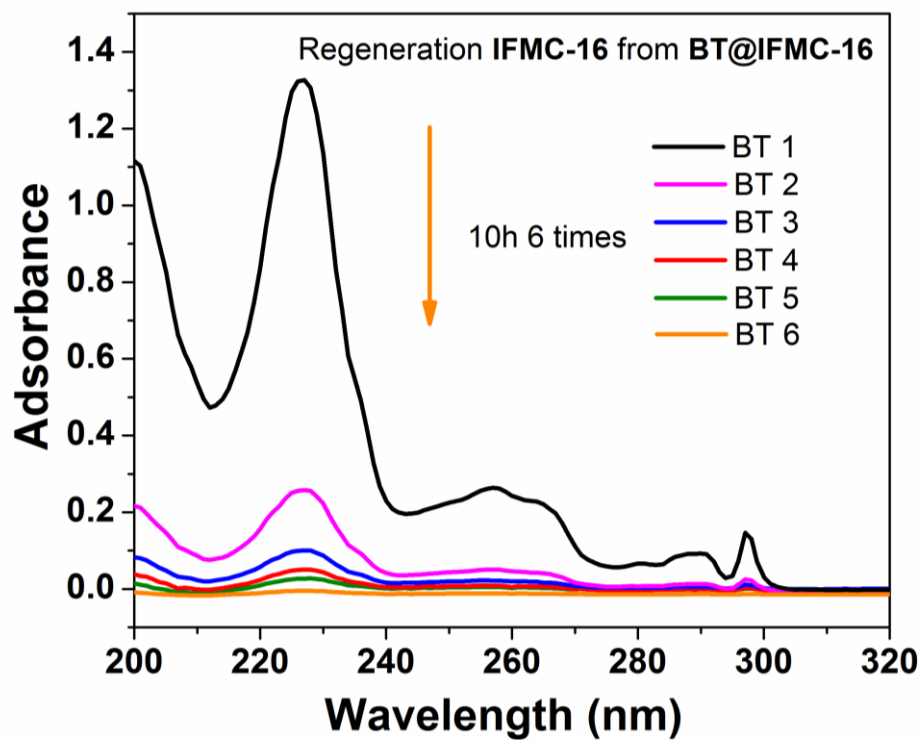
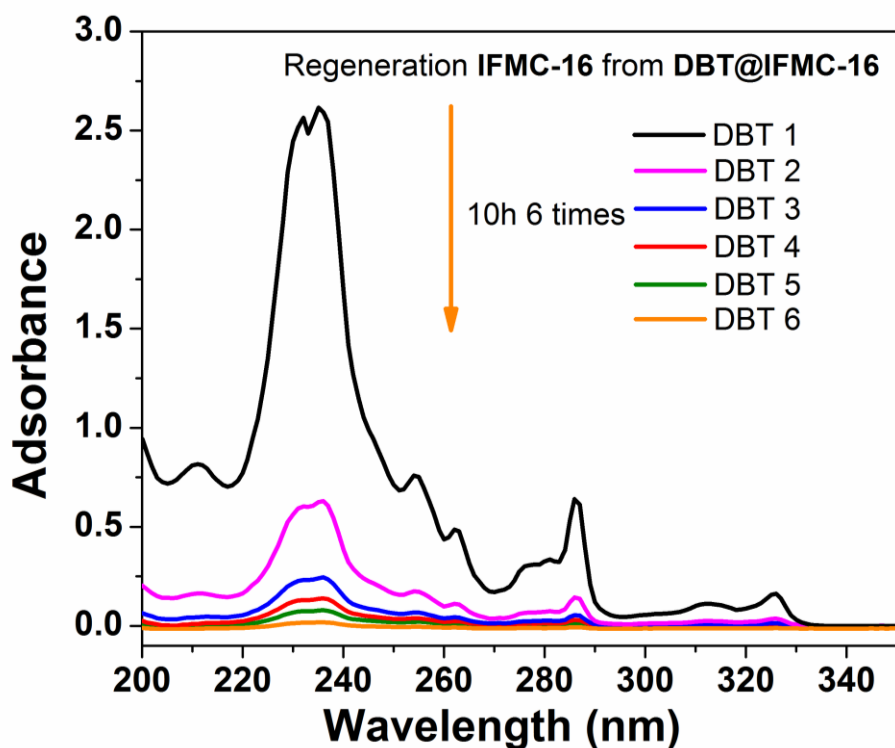


Fig. S13 TGA curves of BT@IFMC-16 (red) and DBT@IFMC-16 (blue).



(a)



(b)

**Fig. S14** UV-Vis spectra for (a) **BT@IFMC-16** and (b) **DBT@IFMC-16** during the regeneration experiments (The spectra correspond to the washed isoctane from top to bottom for 6 times).

The sample of **BT@IFMC-16** or **DBT@IFMC-16** was soaked in isooctane (5 mL), and replaced with fresh isooctane (5 mL) six times in 10 h. The regeneration procedure was monitored by UV/Vis for each washed isooctane. So the “BT1-BT6” stand for the solution of the each washed isooctane, BT1 stands for the solution after soaking the crystals of **BT@IFMC-16** and being replaced for the first time, until BT6 stands for the solution after soaking the crystals of **BT@IFMC-16** and being replaced for the sixth time. So do the symbols “DBT1-DBT6”.

**Table S2** The adsorption amount of **IFMC-16** for BT and DBT in different concentration.

concentration	BT g S kg <sup>-1</sup> MOF	concentration	DBT g S kg <sup>-1</sup> MOF
106 ppmw S	4.97	67 ppmw S	6.17
215 ppmw S	9.85	146 ppmw S	10.45
482 ppmw S	17.91 (17.6) <sup>a</sup>	403 ppmw S	20.93 (19.8) <sup>a</sup>
794 ppmw S	24.44	718 ppmw S	33.92
1059 ppmw S	32.57	1108 ppmw S	41.19
1338 ppmw S	38.70	1361 ppmw S	46.31
1631 ppmw S	47.37	1638 ppmw S	50.58
2045 ppmw S	50.33	1969 ppmw S	54.73

<sup>a</sup> The adsorption amount by using regenerated **IFMC-16**.

**Table S3.** Surface area, pore volume and N<sub>2</sub> uptake for **IFMC-16**, regenerated **IFMC-16**, **BT@IFMC-16** and **DBT@IFMC-16**.

Compound	Surface area [ $\text{m}^2 \cdot \text{g}^{-1}$ ]		$\text{N}_2$ uptake [ $\text{cm}^3 \cdot \text{g}^{-1}$ ]	Pore vol. [ $\text{cm}^3 \cdot \text{g}^{-1}$ ]
	BET	Langmuir		
<b>IFMC-16</b>	2460	2870	670.6	1.037
Regeneration <b>IFMC-16</b> (run 1)	1814	2669	624.8	0.966
Regeneration <b>IFMC-16</b> (run 2)	1798	2651	610.9	0.945
<b>BT@IFMC-16</b> (482 ppmw)	1179	1735	402.3	0.622
<b>DBT@IFMC-16</b> (403 ppmw)	1096	1612	383.1	0.593
<b>BT@IFMC-16</b> (1338 ppmw)	550.4	816.2	224.6	0.347
<b>DBT@IFMC-16</b> (1108 ppmw)	313.7	464.2	129.3	0.200